# Permafrost carbon–climate feedback is sensitive to deep soil carbon decomposability but not deep soil nitrogen dynamics

Charles D. Koven[a,1], David M. Lawrence[b], and William J. Riley[a]

[a]Earth Sciences Division, Lawrence Berkeley National Laboratory, Berkeley, CA 94720; and [b]Climate and Global Dynamics Division, National Center for Atmospheric Research, Boulder, CO 80305

Edited by Inez Y. Fung, University of California, Berkeley, CA, and approved January 30, 2015 (received for review August 8, 2014)

**Permafrost soils contain enormous amounts of organic carbon whose stability is contingent on remaining frozen. With future warming, these soils may release carbon to the atmosphere and act as a positive feedback to climate change. Significant uncertainty remains on the postthaw carbon dynamics of permafrost-affected ecosystems, in particular since most of the carbon resides at depth where decomposition dynamics may differ from surface soils, and since nitrogen mineralized by decomposition may enhance plant growth. Here we show, using a carbon–nitrogen model that includes permafrost processes forced in an unmitigated warming scenario, that the future carbon balance of the permafrost region is highly sensitive to the decomposability of deeper carbon, with the net balance ranging from 21 Pg C to 164 Pg C losses by 2300. Increased soil nitrogen mineralization reduces nutrient limitations, but the impact of deep nitrogen on the carbon budget is small due to enhanced nitrogen availability from warming surface soils and seasonal asynchrony between deeper nitrogen availability and plant nitrogen demands. Although nitrogen dynamics are highly uncertain, the future carbon balance of this region is projected to hinge more on the rate and extent of permafrost thaw and soil decomposition than on enhanced nitrogen availability for vegetation growth resulting from permafrost thaw.**

carbon cycle | Earth system models | cryosphere | soil organic matter | permafrost thaw

As Earth warms in response to human $CO_2$ emissions, a critical uncertainty in the magnitude of expected warming is the degree to which changing climate will lead to changes in the carbon balance of terrestrial ecosystems and thus feed back on climate. High-latitude ecosystems underlain by permafrost soils are a plausible candidate to amplify warming, because they contain an enormous amount of soil organic carbon (1) that is currently stabilized by being frozen or saturated, but may warm and thaw in the future (2). However, high-latitude plant productivity is tightly linked to soil nutrient cycling; in these strongly *N*-limited ecosystems, increases in decomposition may lead to greater N availability and a consequent increase in plant growth that may mitigate C losses (3). Currently, the high latitudes appear to be undergoing a period of carbon cycle intensification characterized by both greater inputs and outputs (4), and central estimates of a synthesis of site-level observations, regional inversion studies, and process models suggest an overall strengthening of the regional C sink (5). Continued warming of these ecosystems will likely be accompanied by continued increases in plant growth and soil C losses; ecosystem models suggest a near cancellation of C gains and losses (6). However, these estimates may underestimate the role of deeper soil C stored in permafrost, whose magnitude is now thought to be larger than earlier estimates suggested (1). Site-based accounting of permafrost C stocks suggests that the quantity of such carbon made vulnerable with warming can be large (7), and that losses from this deep, old C may be the dominant long-term high-latitude response to warming (8).

Most Earth system models (ESMs), which to date have not accounted for many processes associated with thawing permafrost, project high-latitude carbon sinks accompanying warming (9–11). The unique feature of permafrost-affected soils is that there exists a depth beyond which summertime warmth is insufficient to thaw the soil. This limit leads to a separation between surface layers (in which there are both plant-derived C inputs and respiratory losses) and deep layers, which, while they remain frozen, have little C cycle activity but, upon thaw, can potentially have large respiratory losses that are not compensated by inputs (12). Several recent climate-scale land models have included a vertical dimension to soil biogeochemical cycling to resolve depth-dependent changes in soil organic matter (SOM) respiration rates, with either carbon initialization to match soil C maps (13) or via slow mixing by cryoturbation between the seasonally thawed active layers and deeper permafrost layers (14). Including these processes leads to a sign change in the projected high-latitude carbon response to warming, from net C gains driven by increased vegetation productivity and storage resulting from warming and $CO_2$ fertilization to net C losses from enhanced SOM decomposition (13, 15). This qualitative result is supported by simplified permafrost models (7, 16, 17). However, many uncertainties remain on the response magnitude, including (*i*) the extent and rate of physical active layer deepening and permafrost loss with warming (18, 19); (*ii*) the role of water-saturated anoxic soils in reducing $CO_2$ losses (20), increasing $CH_4$ emissions, and generating fine-scale heterogeneity in responses; (*iii*) the degree that N mineralized with decomposing permafrost C can fertilize

## Significance

As the climate warms, the carbon balance of arctic ecosystems will respond in two opposing ways: Plants will grow faster, leading to a carbon sink, while thawing permafrost will lead to decomposition and loss of soil carbon. However, thawing permafrost also releases nitrogen that fertilizes plant growth, offsetting some carbon losses. The balance of these processes determines whether these ecosystems will act as a stabilizing or destabilizing feedback to climate change. We show that this balance is determined by the rate at which permafrost carbon decomposes as it thaws, and that the stabilizing effects of nitrogen from permafrost is weaker than the destabilizing carbon losses from those soil layers.

Author contributions: C.D.K., D.M.L., and W.J.R. designed research; C.D.K. and D.M.L. performed research; C.D.K. and D.M.L. analyzed data; and C.D.K., D.M.L., and W.J.R. wrote the paper.

The authors declare no conflict of interest.

This article is a PNAS Direct Submission.

Freely available online through the PNAS open access option.

[1]To whom correspondence should be addressed. Email: cdkoven@lbl.gov.

This article contains supporting information online at www.pnas.org/lookup/suppl/doi:10.1073/pnas.1415123112/-/DCSupplemental.

plant productivity to offset C losses (21, 22); and (*iv*) the rate and extent to which decomposition occurs in deeper soils after thawing.

The purpose of this paper is to explore the relative magnitudes accompanying warming of carbon losses due to enhanced decomposition versus carbon gains due to increased vegetation productivity in response to elevated $CO_2$ mole fraction, ameliorated growing condition, and N fertilization resulting from enhanced decomposition. In particular, we are interested in the question of how deep SOM initially in permafrost layers may behave after thawing, via its role as both a source of C to the atmosphere and N to stimulate vegetation productivity.

## Materials and Methods

We have included within the Community Land Model, version 4.5 (CLM4.5BGC) (23–27), a basic set of permafrost processes to allow projection of permafrost carbon–climate feedbacks. This model differs from previous permafrost C cycle models by also including a full N cycle, which allows consideration of N limitations on plant productivity, and therefore allows changing soil decomposition to affect productivity via N availability.

Soil C turnover in CLM4.5 is based on a vertical discretization of first-order multipool SOM dynamics (23, 24),

$$\frac{\partial C_i(z)}{\partial t} = R_i(z) + \sum_{i \neq j} (1 - r_j) T_{ji} k_j(z) C_j(z) - k_j(z) C_i(z) + \frac{\partial}{\partial z}\left(D(z)\frac{\partial C_i}{\partial z}\right) + \frac{\partial}{\partial z}(A(z)C_i),$$

where $C_i$ is the carbon in pool $i$ at vertical level $z$, $R_i$ are the carbon inputs to pool $i$, $T_{ji}$ is a transfer matrix of decomposition from pool $j$ to pool $i$, $k_i$ is the decay constant of pool $i$, and $D$ and $A$ represent vertical transport by diffusion and advection, respectively. The $k_i$ is modified by the soil environment for all pools,

$$k_i = k_{0,i} r_T r_W r_O r_z,$$

with $k_{0,i}$ an intrinsic, pool-specific rate, $r_T$ the direct temperature control ($Q_{10} = 1.5$), $r_w$ the liquid moisture control, $r_O$ the oxygen control, and $r_z$ the direct depth control, which is defined as

$$r_z = \exp\left(-\frac{z}{z_\tau}\right)$$

with $Z_\tau$ a depth control parameter discussed below. We use a vertical grid with 30 levels that has a high-resolution exponential grid in the interval 0–0.5 m and fixed 20-cm layer thickness in the range of 0.5–3.5 m to maintain resolution through the base of the active layer and upper permafrost, and reverts to exponentially increasing layer thickness in the range 3.5–45 m to allow for large thermal inertia at depth. All other parameters are as listed in ref. 24.

To understand the role of N cycle in mediating C cycle responses, we define a C-only model, following the approach of ref. 28, in which gross primary productivity (GPP) is not limited by soil mineral nitrogen, but instead each Plant Functional Type (PFT) has a constant fractional reduction in the rate of photosynthesis to give equivalent preindustrial net primary productivity (NPP). This reduction is calculated by finding the time-constant N limitation factor for each PFT that gives the same total PFT-integrated NPP for preindustrial conditions (repeating 1901–1920 meteorology, 1850 $CO_2$) as the coupled C–N model (*SI Appendix*, Table S1).

Our experimental design is an offline analog to a Coupled Carbon Cycle Climate Model Intercomparison Project ($C^4$MIP) experimental setup (29) under an unmitigated $CO_2$ increase scenario, and includes (*i*) control; (*ii*) biogeochemically forced, i.e., plants experience the physiological effects of elevated $CO_2$ while climate is not impacted by $CO_2$ radiative effects; (*iii*) climatically forced, i.e., ecosystems respond to warming but not the physiological effects of $CO_2$; and (*iv*) fully forced, so that both physiological and climate effects of increasing $CO_2$ are considered. Land use and N deposition are identical for all cases.

We force CLM4.5BGC with time-varying meteorology, $CO_2$ concentration, N deposition, and land use change to estimate the C cycle response to global change. The atmospheric forcing data for 1850–2005 are taken from the combined Climatic Research Unit and National Center for Environment Predication (CRUNCEP) dataset (data available at dods.ipsl.jussieu.fr/igcmg/IGCM/BC/OOL/OL/CRU-NCEP/), which merges high-frequency variability from the National Centers for Environmental Prediction–National Center for Atmospheric Research reanalysis (30) with the monthly mean climatologies from the CRU temperature and precipitation datasets (31). Projection period forcing is calculated by applying monthly climate anomalies/scale factors from a Community Earth System Model, version 1 (CESM1) simulation for the scenarios Representative Concentration Pathway 8.5 (RCP8.5) for the years 2006–2100 and Extended Concentration Pathway 8.5 (ECP8.5) for the years 2100–2300 to repeating 1996–2005 CRUNCEP meteorology. For constant climate (control and biogeochemically forced) runs, atmospheric data are repeated over the period 1901–1920. $CO_2$ concentrations follow transient historical (1850–2005), RCP8.5 (2006–2100), and ECP8.5 (2101–2300) concentrations for biogeochemically and fully forced runs, and remain fixed at 1850 levels (284.7 ppm) for control and climatically forced runs. Atmospheric N deposition is from coupled atmospheric chemistry–climate runs (32), land use follows the historical (1850–2005) and RCP8.5 (2006–2100) scenarios (33), and both are transient in all cases. After 2100, land use is static and wood harvest is zero.

We consider sensitivity of the model to two separate processes: N modulation of C cycle feedbacks and the role of deep versus shallow SOM. To examine N control on C cycle feedbacks, we compare the C–N and C-only model configurations discussed above.

To understand the role of deep versus shallow C, we vary the decomposability of deep C in the model. As discussed above, heterotrophic respiration (HR) is limited in CLM4.5 by temperature, moisture, and oxygen (resolved controls). Our previous work with CLM4.5 showed that these resolved controls are insufficient to predict both observed total C and $^{14}$C SOM profiles in temperate soils (23). This result is consistent with some (34), but not all (35), recent modeling analyses using similar vertically resolved carbon decomposition models. To address this issue, we defined in CLM4.5 an e-folding distance, $Z_\tau$, that modifies HR by decreasing the respiration flux from each pool as an exponential function of depth (23). This depth control of HR is intended to represent net impacts of soil microbial controls, pore-scale oxygen transport, mineral sorption, priming effects, aggregation, and other unresolved processes, which observations suggest reduce decomposition rates at depth beyond the limitations of temperature, moisture, and bulk oxygen availability (36, 37). To the extent that such direct depth effects are due to long-term processes such as limitation by microbial activity or priming, they may not apply to highly nonequilibrium cases such as thawing permafrost, and because there is a large amount of SOM C in the 1- to 3-m depth interval in permafrost regions (1, 7), the decomposability of this carbon to warming represents a potentially important feedback with climate. We explore the sensitivity of the permafrost carbon–climate feedback to vertical (0–3 m) gradients in soil decomposability with a perturbed parameter experiment, comparing cases with high ($Z_\tau = 0.5$ m), medium ($Z_\tau = 1$ m), and low ($Z_\tau = 10$ m) additional limitation on decomposition with depth.

A recent model intercomparison (38) highlighted the large uncertainties in a broad suite of terrestrial carbon cycle models. We note that the model used here (CLM4.5) was not present in that intercomparison but does perform relatively well compared with the FLUXNET (39) estimates for GPP (*SI Appendix*, Fig. S1). We also not that, while CLM does include the hydrological impedance of drainage by permafrost (27), it does not include subgridscale heterogeneity in soil moisture, and therefore may overestimate overall respiration rates as it does not maintain a fully saturated fraction of grid cells.

## Results and Discussion

The imposed warming leads to large losses of near-surface permafrost area and volume by 2300 (Fig. 1*A* and *SI Appendix*, Fig. S2); most of the thaw occurs in the period 2050–2150, which is somewhat delayed relative to losses seen in fully coupled land–atmosphere modeling experiments using an earlier version of CLM (40). This relative delay is due partially to our use here of observationally derived atmospheric forcing data, which leads to colder simulated preindustrial soil temperatures. Taking the mean across the permafrost domain, defined as areas initially having permafrost within 3 m of the surface, the environmental changes have a strong effect on soil decomposition rates (Fig. 2 *A*–*D*). The direct temperature effect is modest, as the temperature control is represented with a $Q_{10}$ value of 1.5. The stronger controls on SOM turnover are liquid moisture availability, which is a function of unfrozen water content and therefore is sharply increased when soils thaw, and oxygen, which becomes a weaker limitation when permafrost thaws and water is able to drain from the soil. The product of these terms thus reverses its vertical profile from the initial period in which decomposition proceeds more slowly at depth (in permafrost) than at the surface (active layer) to one in which decomposition proceeds more rapidly at depth (in perennially thawed talik) than at the surface (seasonally frozen ground).



ENVIRONMENTAL SCIENCES

EARTH, ATMOSPHERIC, AND PLANETARY SCIENCES

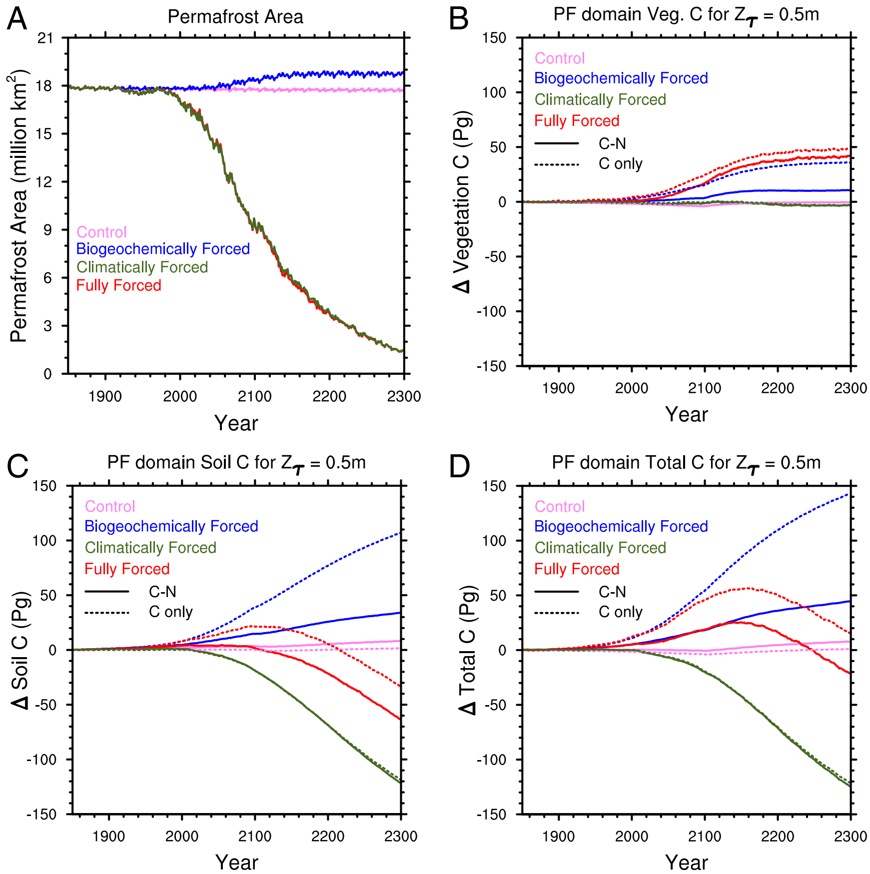


**Fig. 1.** CLM near-surface permafrost area and C stock responses to forcings (combinations of changing vs. fixed $CO_2$ and climate), and model configurations (C only and combined C–N) for the case with relatively insensitive deep C ($Z_\tau$ = 0.5 m). (*A*) Near-surface permafrost area, defined as area with permafrost simulated in upper 3 m of soil. (*B*) Change in vegetation C over the permafrost region. Increase in vegetation C at 2100 is due to a discontinuation of wood harvest after the end of the RCP8.5 land use dataset and occurs in all cases. (*C*) Change in total C of the permafrost region, defined as the geographic area with permafrost in upper 3 m for 1850–1900 period. (*D*) Change in soil and litter C over permafrost domain. The solid and dashed lines represent the coupled carbon and nitrogen simulation and the carbon-only simulation, respectively.

In the climatically forced simulation with strongly inhibited decomposition at depth ($Z_\tau$ = 0.5 m), vegetation C initially increases relative to the control run due to improving growing conditions (Fig. 1*B*). As warming progresses, vegetation C is lost starting around 2100 due to increasing fire frequency in the boreal zone. The projected vegetation response to $CO_2$ shows that the permafrost domain is highly N limited, and thus the vegetation C in the coupled C–N model responds only weakly to the physiological effects of increased $CO_2$ concentration alone compared with the C-only model, but that under the combined effects of warming and elevated $CO_2$, much of this limitation is removed due to additional N released by mineralization of decomposing SOM primarily near the surface (as discussed below). Thus, there is a strong N-mediated synergistic effect between warming and $CO_2$ fertilization (41),

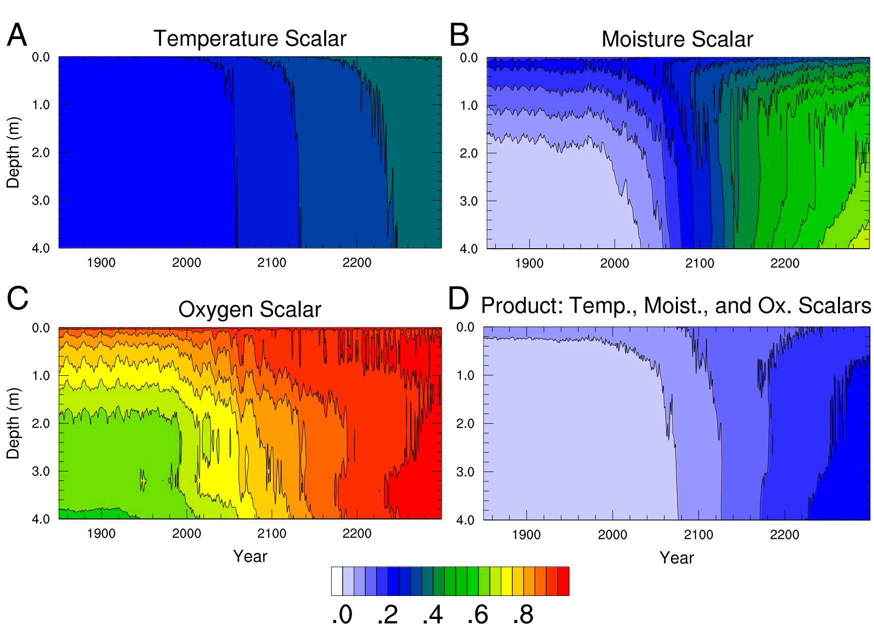


**Fig. 2.** Soil decomposition environmental rate scalar values in the fully forced run, annual mean and averaged over the permafrost region, shown as a function of depth and time: (*A*) temperature scalar, (*B*) liquid moisture scalar, (*C*) oxygen scalar, and (*D*) the product of these three environmental controls on decomposition. The primary limitation to decomposition associated with freezing is via the moisture scalar; thus it shows the strongest change in magnitude and vertical profile with warming and thawing.

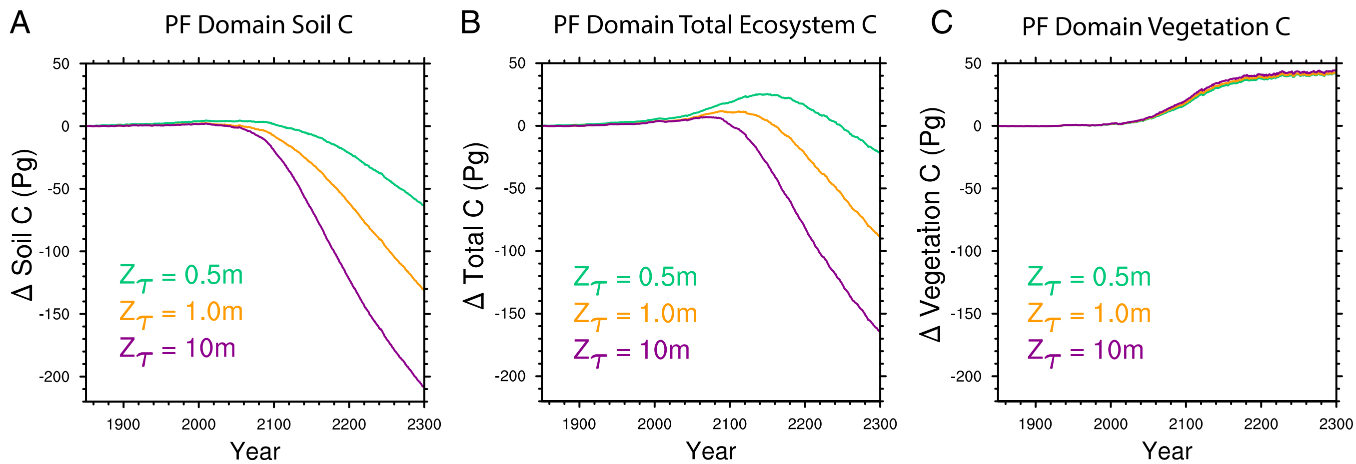


**Fig. 3.** C response to decomposability of deep C in the fully forced C–N case. (*A*) Soil and litter C changes over the permafrost region. (*B*) Change in total ecosystem C as a function of varied $Z_\tau$ parameter. (*C*) Change in vegetation C. Slight increase in vegetation between cases is due to enhanced N mineralization from deep soils.

leading the fully forced C–N model to behave similarly to the C-only model for total ecosystem carbon: Carbon gains by enhanced vegetation growth are offset by SOM losses from shallow soils (Fig. 1*C*), leading to only a small residual sink (in the C-only case) or source (in the C–N case) by 2300 (Fig. 1*D*).

Allowing decomposition to proceed more rapidly at depth by increasing the value of $Z_\tau$ results in less preindustrial soil carbon throughout the permafrost region (*SI Appendix*, Fig. S3; 1,582 Pg for $Z_\tau = 0.5$ m, 1,331 Pg for $Z_\tau = 1.0$ m, and 1,032 Pg for $Z_\tau = 10$ m, compared with 29–30 Pg C in vegetation C). This reduction in initial C is due to higher decomposition rates at depth during the model initialization period, and the lower stock (higher value of $Z_\tau$) is in better agreement with estimates of integrated permafrost C to 3 m from observations [1,060 Pg C (7)]. As $Z_\tau$ increases, the deeper soil carbon is much more vulnerable to loss with warming (Fig. 3*A*), so that by 2300, the total C loss from the region is 164 Pg for $Z_\tau = 10$ m compared with 21 Pg for $Z_\tau = 0.5$ m (Fig. 3*B*).

The additional N released from deeper SOM turnover has only a small effect on plant productivity, with <5 Pg additional increase in vegetation C for $Z_\tau = 10$ m compared with $Z_\tau = 0.5$ m (relative to ∼40 Pg C increase by 2300, Fig. 3*C*). This small sensitivity of vegetation to deep soil N mineralization has two causes: (*i*) Much of the N limitation is already relieved by increased decomposition in surface soils, and (*ii*) the phase lag of heat conduction shifts the deeper SOM mineralization later into fall and winter, away from the period of peak N demand during the high-GPP spring and summer periods (Fig. 4). This seasonal offset allows a greater fraction of N to be lost via leaching and gaseous loss pathways. These losses are consistent with observations showing that the highest dissolved losses from arctic ecosystems occur during the spring meltwater pulse (42). We note that CLM4.5 does not currently represent the complexity of soil microbial N cycling found in response to experimental winter warming treatments (43). The large amount of N released, particularly if not used by plants, may have significant impacts, such as on N trace gases (44) and aquatic ecosystems. We emphasize that the representation of such N cycle processes are particularly uncertain in models such as CLM, and thus this result serves primarily to underscore the importance of these processes in governing C cycle responses to warming.

At the regional scale, the projected timing of permafrost C losses is delayed relative to physical permafrost thaw; while about half the permafrost area has fully thawed by 2100, the permafrost soil C losses in the fully forced scenario are only beginning then. This regional response is the aggregate of different dynamics at the scale of individual grid cells (Fig. 5). Typical trajectories for the $Z_\tau = 10$ m case are that grid cells are initially

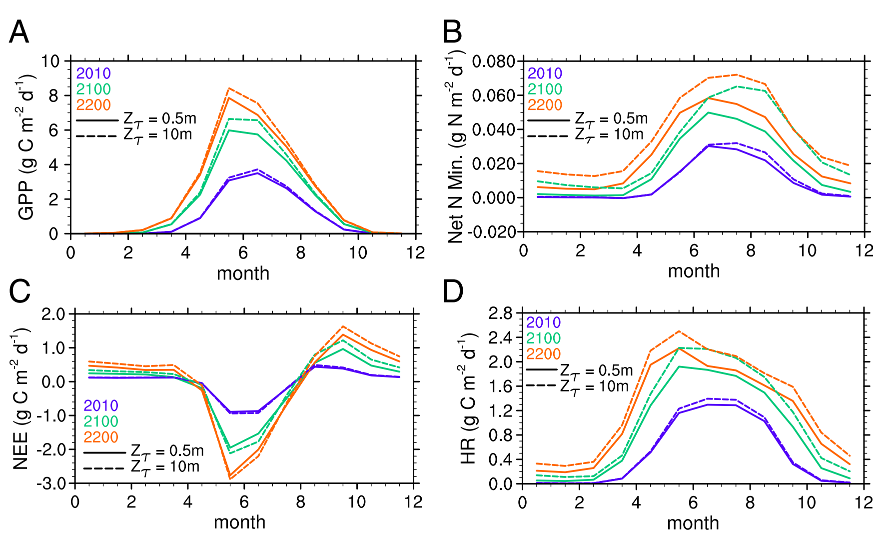


**Fig. 4.** Mean annual cycles of key ecosystem fluxes for three time periods of the fully forced C–N case. (*A*) GPP, (*B*) net N mineralization, (*C*) net ecosystem exchange (NEE, positive = $CO_2$ source), and (*D*) heterotrophic respiration. Relative increase in GPP between experiments is smaller than proportional increase in N mineralization with deeper decomposition. Shift in N mineralization with enhanced deeper SOM decomposition toward autumn is due to longer decomposing than growing seasons, and phase lag of temperature in deep soils. The solid and dashed lines represent $Z_\tau = 0.5$ m and 10 m, respectively. All cases show the mean of the geographic region in which permafrost initially occurs in the model.

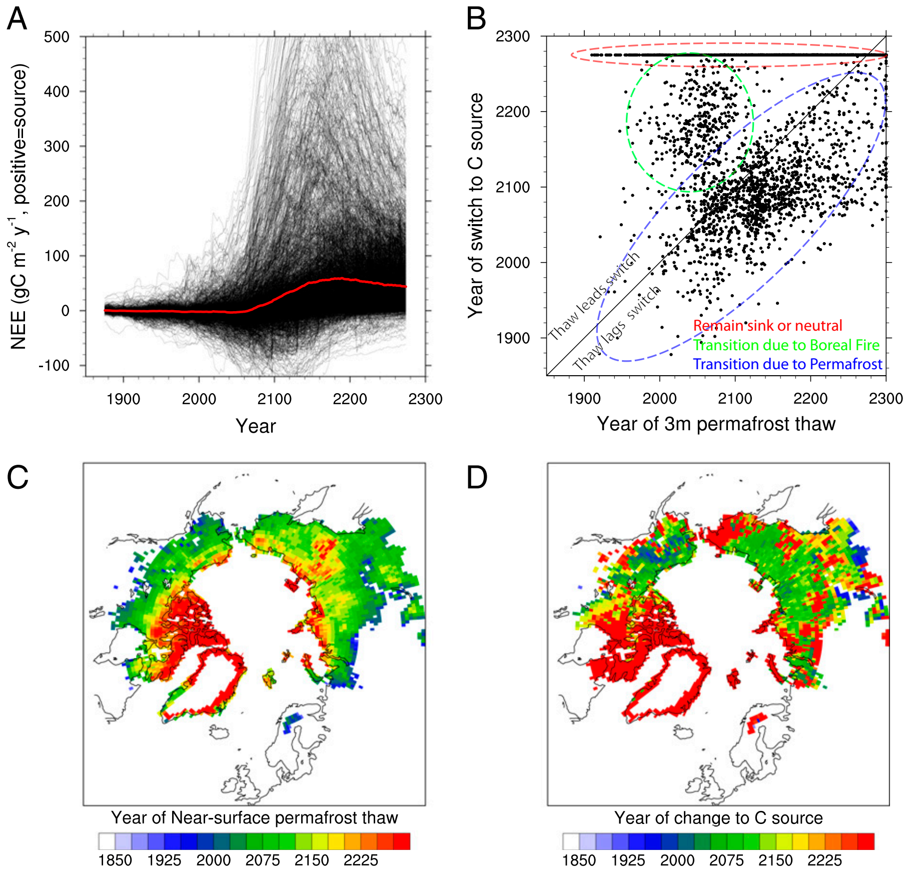


**Fig. 5.** Timing of C balance and permafrost thaw. (*A*) Trajectories of 50-y smoothed carbon balance for all grid cells in permafrost region. The regional mean trajectory (red line in *A*) begins as a C sink, then switches to a source; individual grid cells (thin black lines) begin as either neutral or C sinks, and then some of these transition to sources. Here we define source transition timing as the year in which the smoothed C flux exceeds 25 gC·m$^{-2}$·y$^{-1}$. (*B*) Comparison of thaw year against C sink transition year for each grid cell. (*C*) Year in which the permafrost thaws at each grid cell to a depth of at least 3 m; red grid cells do not thaw to that depth during the simulation. (*D*) Year of source transition; red grid cells do not become sources of at least 25 gC·m$^{-2}$·y$^{-1}$ at any time during the experiment. Grid cells in *B* fall into three groups: (red) the line of cells at the top that do not transition from sink to source; (blue) a main trend of permafrost-dominated grid cells, in which transition from sink to source generally leads the thaw of permafrost to 3m depth; and (green) a smaller set of grid cells that transition from sink to source after thaw due to increased boreal fire rather than permafrost processes.

neutral or sinks, and then switch to become sources when SOM decomposition exceeds vegetation productivity. Although some grid cells either do not transition to sources or do so due to boreal forest processes (principally fire), the main group of permafrost-dominated grid cells transition before a 3-m thaw depth, suggesting that initial active layer deepening is sufficient for a source transition. Once decomposition-driven C losses overtake growth-driven gains, C losses persist long after the soils have thawed (*SI Appendix*, Fig. S4 and Movie S1).

The direct C loss due to climate forcing alone in the presence of elevated $CO_2$ (i.e., fully forced minus biogeochemically forced) ranges from 66 Pg ($Z_\tau = 0.5$ m) to 207 Pg ($Z_\tau = 10$ m), corresponding to a permafrost region feedback factor, γ (10), of 7.3–23 Pg C·K$^{-1}$ [corresponding to 0.04–0.11 W m$^{-2}$·K$^{-1}$ (45)] given the global mean 9 °C projected warming. For ΔT, we use the global mean of the anomaly forcing over the period 2005–2300, plus the observed 20th century warming in the CRU dataset (which determines the temperature trends over the historical period in the forcing data). This feedback factor shows a threshold response with essentially no feedback until global ΔT exceeds 4 °C and increasing rapidly afterward (*SI Appendix*, Fig. S5). The permafrost γ calculated here is at the low end of the range estimated in Intergovernmental Panel on Climate Change Fifth Assessment Report (IPCC-AR5) (9) based on simplified models; this is partly because we include both vegetation growth and a set of stabilizing responses, including the synergistic N mineralization and elevated $CO_2$ effects, within this estimate.

In addition to direct C cycle feedbacks, there is widespread interest in the greenhouse gas contribution of $CH_4$ emissions from thawing permafrost. The additional and deeper decomposition projected here leads to slightly higher $CH_4$ emissions (∼+10 Tg $CH_4$−C·y$^{-1}$ with $Z_\tau = 10$ m versus $Z_\tau = 0.5$ m, which equates to ∼90 Tg $CO_2$−C·yr$^{-1}$ equivalent, assuming a global warming potential (GWP) of 25; *SI Appendix*, Fig. S6), but these emissions would contribute only a small extra warming compared with the increased $CO_2$ emissions (∼+900 Tg C·yr$^{-1}$ $CO_2$ emissions in $Z_\tau = 10$ m versus $Z_\tau = 0.5$ m during 22nd century). We note that projected $CH_4$ emissions, and their sensitivity to climate forcing, are highly uncertain (25).

Comparing the control of ecosystem C feedbacks by deep soil decomposability over the permafrost domain compared with the mean of the rest of the world where permafrost is not initially present (*SI Appendix*, Figs. S7 and S8) shows that the permafrost region is the primary area in which decomposition dynamics under warming are qualitatively different at depth than at the surface, and thus is the primary region where allowing deep C cycling to proceed rapidly ($Z_\tau = 10$ m) vs. slowly ($Z_\tau = 0.5$ m) has a strong effect on the projected overall C budget.

Large uncertainties remain in the ability to project permafrost C losses in particular, and high-latitude ecosystem C responses to climate change in general. Arctic ecosystems are complex, and poorly represented in global-scale terrestrial carbon cycle models (38). The results shown here, that highly divergent responses arise from plausibly different decomposition dynamics in deep soils, demonstrate a need to focus on the mechanistic controls of decomposition (e.g., microbial community dynamics, mineral surface interactions, root interactions) in thawing permafrost. Observations of rapid microbial community adjustment and utilization of frozen carbon (46), and comparable C loss rates during incubation of SOM from shallow versus deep soil layers in permafrost-affected soils (47), suggest that decomposition dynamics may be highly dynamic and thus follow more closely the $Z_\tau = 10$ m scenario outlined here. However, many relevant processes are still poorly represented in CLM and analogous models; these include the use of static vegetation distributions and simple vegetation community definitions, poor knowledge of complex C–N interactions such as gaseous and dissolved N losses, plant N uptake and storage dynamics, fine-scale processes such as polygon dynamics and heterogeneous thaw processes including the possibility of rapid carbon mobilization due to thermokarst, and biogeophysical climate feedbacks, in addition to the overarching uncertainties in permafrost thaw rates and soil C dynamics. Reducing these uncertainties will require experimental designs to measure coupled C and N dynamics during thaw progression to better understand both the decomposability of permafrost C and how the N mineralized during decomposition affects ecosystem productivity.

The results presented here—that large C losses are possible from the permafrost region, whose magnitude is strongly governed by the dynamics of deeper decomposition, and that large losses are unlikely to be compensated by N fertilization accompanying decomposition—underscore the importance of considering permafrost carbon dynamics in ESMs. Permafrost soils may produce a strong, albeit delayed, C response to global change, and must therefore be included in assessments of long-term C cycle feedbacks to climate change.

**ACKNOWLEDGMENTS.** This research was supported by the Director, Office of Science, Office of Biological and Environmental Research of the US Department of Energy (DOE) under Contract DE-AC02-05CH11231 as part of their Earth System Modeling, Regional and Global Climate Modeling, and Terrestrial Ecosystem Science Programs and used resources of the National Energy Research Scientific Computing Center, also supported by the Office of Science of the US Department of Energy, under Contract DE-AC02-05CH11231. The Next-Generation Ecosystem Experiments (NGEE Arctic) project is supported by the Office of Biological and Environmental Research in the DOE Office of Science. National Center for Atmospheric Research (NCAR) is sponsored by the National Science Foundation (NSF). The CESM project is supported by the NSF and the Office of Science (BER) of the US Department of Energy. Computing resources were provided by the Climate Simulation Laboratory at NCAR's Computational and Information Systems Laboratory, sponsored by NSF and other agencies. D.M.L. is supported by funding from the US Department of Energy BER, as part of its Climate Change Prediction Program, Cooperative Agreement DE-FC03-97ER62402/A010 and NSF Grants AGS-1048996 and ARC-1048987.

1. Tarnocai C, et al. (2009) Soil organic carbon pools in the northern circumpolar permafrost region. *Glob Biogeochem Cycles* 23(2):GB2023.
2. Goulden ML, et al. (1998) Sensitivity of boreal forest carbon balance to soil thaw. *Science* 279(5348):214–217.
3. Shaver GR, et al. (1992) Global change and the carbon balance of Arctic Ecosystems. *Bioscience* 42(6):433–441.
4. Graven HD, et al. (2013) Enhanced seasonal exchange of $CO_2$ by northern ecosystems since 1960. *Science* 341(6150):1085–1089.
5. McGuire AD, et al. (2012) An assessment of the carbon balance of Arctic tundra: Comparisons among observations, process models, and atmospheric inversions. *Biogeosciences* 9(8):3185–3204.
6. Euskirchen ES, McGuire AD, Chapin FS, 3rd, Yi S, Thompson CC (2009) Changes in vegetation in northern Alaska under scenarios of climate change, 2003–2100: Implications for climate feedbacks. *Ecol Appl* 19(4):1022–1043.
7. Harden JW, et al. (2012) Field information links permafrost carbon to physical vulnerabilities of thawing. *Geophys Res Lett* 39(15):L15704.
8. Schuur EAG, et al. (2009) The effect of permafrost thaw on old carbon release and net carbon exchange from tundra. *Nature* 459(7246):556–559.
9. Ciais P, et al. (2013) *Climate Change 2013: The Physical Science Basis. Contribution of Working Group I to the Fifth Assessment Report of the Intergovernmental Panel on Climate Change*, eds Stocker TF, et al. (Cambridge Univ Press, Cambridge, UK).
10. Friedlingstein P, et al. (2006) Climate–carbon cycle feedback analysis: Results from the C4MIP Model Intercomparison. *J Clim* 19(14):3337–3353.
11. Qian H, Joseph R, Zeng N (2010) Enhanced terrestrial carbon uptake in the northern high latitudes in the 21st century from the Coupled Carbon Cycle Climate Model Intercomparison Project model projections. *Glob Change Biol* 16(2):641–656.
12. Rapalee G, Trumbore SE, Davidson EA, Harden JW, Veldhuis H (1998) Soil carbon stocks and their rates of accumulation and loss in a boreal forest landscape. *Glob Biogeochem Cycles* 12(4):687–701.
13. Schaefer K, Zhang T, Bruhwiler L, Barrett AP (2011) Amount and timing of permafrost carbon release in response to climate warming. *Tellus B Chem Phys Meterol* 63(2):165–180.
14. Koven CD, et al. (2009) On the formation of high-latitude soil carbon stocks: The effects of cryoturbation and insulation by organic matter in a land surface model. *Geophys Res Lett* 36(21):L21501.
15. Koven CD, et al. (2011) Permafrost carbon-climate feedbacks accelerate global warming. *Proc Natl Acad Sci USA* 108(36):14769–14774.
16. Burke EJ, Hartley IP, Jones CD (2012) Uncertainties in the global temperature change caused by carbon release from permafrost thawing. *Cryosphere Discuss* 6(2):1367–1404.
17. Schneider von Deimling T, et al. (2012) Estimating the near-surface permafrost-carbon feedback on global warming. *Biogeosciences* 9(2):649–665.
18. Slater AG, Lawrence DM (2013) Diagnosing present and future permafrost from climate models. *J Clim* 26(15):5608–5623.
19. Koven CD, Riley WJ, Stern A (2012) Analysis of permafrost thermal dynamics and response to climate change in the CMIP5 Earth System Models. *J Clim* 26(6):1877–1900.
20. Elberling B, et al. (2013) Long-term $CO_2$ production following permafrost thaw. *Nat Clim Change* 3:890–894.
21. Keuper F, et al. (2012) A frozen feast: Thawing permafrost increases plant-available nitrogen in subarctic peatlands. *Glob Change Biol* 18(6):1998–2007.
22. Waelbroeck C, Monfray P, Oechel W, Hastings S, Vourlitis G (1997) The impact of permafrost thawing on the carbon dynamics of tundra. *Geophys Res Lett* 24(3):229–232.
23. Koven CD, et al. (2013) The effect of vertically-resolved soil biogeochemistry and alternate soil C and N models on C dynamics of CLM4. *Biogeosci Discuss* 10(4):7201–7256.
24. Oleson KW, et al. (2013) *Technical Description of Version 4.5 of the Community Land Model (CLM)* (Natl Cent Atmos Res, Boulder, CO).
25. Riley WJ, et al. (2011) Barriers to predicting changes in global terrestrial methane fluxes: Analyses using CLM4Me, a methane biogeochemistry model integrated in CESM. *Biogeosciences* 8(1):1925–1953.
26. Swenson SC, Lawrence DM (2012) A new fractional snow-covered area parameterization for the Community Land Model and its effect on the surface energy balance. *J Geophys Res* 117(D21):D21107.
27. Swenson SC, Lawrence DM, Lee H (2012) Improved simulation of the terrestrial hydrological cycle in permafrost regions by the Community Land Model. *J Adv Model Earth Syst* 4(3):M08002.
28. Bonan GB, Levis S (2010) Quantifying carbon-nitrogen feedbacks in the Community Land Model (CLM4). *Geophys Res Lett* 37(7):L07401.
29. Arora VK, et al. (2013) Carbon-concentration and carbon-climate feedbacks in CMIP5 Earth system models. *J Clim* 26(15):5289–5314.
30. Kalnay E, et al. (1996) The NCEP/NCAR 40-year reanalysis project. *Bull Am Meteorol Soc* 77(3):437–471.
31. Harris I, Jones PD, Osborn TJ, Lister DH (2014) Updated high-resolution grids of monthly climatic observations – the CRU TS3.10 Dataset. *Int J Climatol* 34(3):623–642.
32. Lamarque J-F, et al. (2010) Historical (1850–2000) gridded anthropogenic and biomass burning emissions of reactive gases and aerosols: Methodology and application. *Atmos Chem Phys* 10(15):7017–7039.
33. Lawrence PJ, et al. (2012) Simulating the biogeochemical and biogeophysical impacts of transient land cover change and wood harvest in the Community Climate System Model (CCSM4) from 1850 to 2100. *J Clim* 25(9):3071–3095.
34. Jenkinson D, Coleman K (2008) The turnover of organic carbon in subsoils. Part 2. Modelling carbon turnover. *Eur J Soil Sci* 59(2):400–413.
35. Braakhekke MC, et al. (2014) The use of radiocarbon to constrain current and future soil organic matter turnover and transport in a temperate forest. *J Geophys Res* 119(3):372–391.
36. Schmidt MWI, et al. (2011) Persistence of soil organic matter as an ecosystem property. *Nature* 478(7367):49–56.
37. Carrasco JJ, Neff JC, Harden JW (2006) Modeling physical and biogeochemical controls over carbon accumulation in a boreal forest soil. *J Geophys Res* 111(G2):G02004.
38. Fisher JB, et al. (2014) Carbon cycle uncertainty in the Alaskan Arctic. *Biogeosciences* 11(15):4271–4288.
39. Beer C, et al. (2010) Terrestrial gross carbon dioxide uptake: Global distribution and covariation with climate. *Science* 329(5993):834–838.
40. Lawrence DM, Slater AG, Swenson SC (2012) Simulation of present-day and future permafrost and seasonally frozen ground conditions in CCSM4. *J Clim* 25(7):2207–2225.
41. Mahecha MD, et al. (2010) Comparing observations and process-based simulations of biosphere-atmosphere exchanges on multiple timescales. *J Geophys Res* 115(G2):G02003.
42. Neff JC, Hooper DU (2002) Vegetation and climate controls on potential $CO_2$, DOC and DON production in northern latitude soils. *Glob Change Biol* 8(9):872–884.
43. Schimel JP, Bilbrough C, Welker JA (2004) Increased snow depth affects microbial activity and nitrogen mineralization in two Arctic tundra communities. *Soil Biol Biochem* 36(2):217–227.
44. Repo ME, et al. (2009) Large $N_2O$ emissions from cryoturbated peat soil in tundra. *Nat Geosci* 2:189–192.
45. Gregory JM, Jones CD, Cadule P, Friedlingstein P (2009) Quantifying carbon cycle feedbacks. *J Clim* 22(19):5232–5250.
46. Mackelprang R, et al. (2011) Metagenomic analysis of a permafrost microbial community reveals a rapid response to thaw. *Nature* 480(7377):368–371.
47. Schädel C, et al. (2014) Circumpolar assessment of permafrost C quality and its vulnerability over time using long-term incubation data. *Glob Change Biol* 20(2):641–652.